The transmission of SARS-CoV-2 is likely comodulated by temperature and by relative humidity

Kevin S. Raines[1], Sebastian Doniach[2], Gyan Bhanot[3 4 5 6]

[1] kevin.raines@protonmail.com

[2]Applied Physics, McCullough 308, Stanford University, Stanford, CA, 94305

[3]Department of Molecular Biology and Biochemistry, Rutgers University, Piscataway, NJ, 08854, USA

[4]Department of Physics and Astronomy, Rutgers University, Piscataway, NJ, 08854, USA

[5]Rutgers Cancer Institute of New Jersey, New Brunswick, NJ, 08903, USA

[6]School of Medicine, University of California San Diego, La Jolla, CA 92093, USA

May 23, 2020

Abstract

Quantifying the role of temperature and humidity on the transmission of SARS-CoV-2 has been confounded by a lack of controlled experiments, the sudden rise in detection rates, and changing weather patterns. In this paper we focus our analysis on data from Colombia, which presents unique economic, demographic and geological characteristics that favor the study of temperature and humidity upon SARS-CoV-2 transmission: the weather varies dramatically across five natural regions (from the Caribbean coast and the Amazon rainforest to the Andean mountains), there are no pronounced seasons, there is a central port of entry, the use of public transportation dominates inter- and intracity travel, and indoor climate control is rare. While only controlled experiments can precisely quantify the role of temperature and humidity upon SARS-CoV-2 transmission, we observe significant attenuation of transmission in climates with sustained daily maximum temperatures above 30 degrees Celsius and simultaneous mean relative humidity below 78%. We hypothesize that temperature and relative humidity comodulate the infectivity of SARS-CoV-2 within respiratory droplets.

Keywords:SARS-CoV-2 seasonality, Covid-19 weather, SARS-CoV-2 epidemiology, SARS-CoV-2 temperature, SARS-CoV-2 relative humidity

1 Introduction

Coronaviruses are a class of large, enveloped, single-strand RNA viruses that are widespread in animals and provoke respiratory illnesses in humans [1] [2]. The novel coronavirus SARS-CoV-2 was identified in January 2020 as the likely causative agent of a cluster of pneumonia cases appearing in Wuhan, China throughout December 2019, making it the seventh known coronavirus to cause pathology in humans [1]. SARS-CoV-2 is associated with a respiratory illness, Covid-19, that ranges in severity from a symptomless infection [3], to common-cold like symptoms, to viral pneumonia, acute respiratory distress syndrome (ARDS), and death [4] [5] [6] [7]. While the mortality in SARS-CoV-2 appears to be lower than in SARS-CoV [5], this new virus has more favorable transmission characteristics, including an asymptomatic infective phase [8] [9] [10] [11] [12] [13] [14] [15].

From early January to March 2020, SARS-CoV-2 quickly spread around the world causing a global pandemic [16]. While global data will certainly play a role in elucidating the epidemiology of Covid-19, we have identified three factors that confound global data: (1) asynchronous and varied responses by local and national governments [17] [18] (2) regional variations in disease awareness, testing protocols, and testing kit-availability leading to disparate and dynamic disease detection rates [19] [20] and (3) unknown variations in the rate at which infectious travelers carried the disease into local populations [21]. In other words, varied responses by governments, from total quarantine to vague social distancing suggestions, dynamic detection rates (see figure 1) and varying rates at which the disease was introduced into each locale suggest that by-nation or even by-city analyses are necessary to control for the above factors. Moreover, changing seasons in the hemispheres during the spread of the pandemic further confounds the analysis of weather factors from global data.

In order to mitigate these factors, we conducted a by-city analysis on Colombian data and we developed an appropriate data model. Colombia is uniquely suited for the study of weather factors on the transmission of SARS-CoV-2 for the following five reasons:

1. *Climate variation.* Colombia has five geographically distinct regions [22]: the Pacific coastal region, the Caribbean coastal region, the Andean mountain region, *los llanos* (grassland plains), and the Amazon Rainforest region. Seasons are a known confounding factor in the analysis of weather factors in transmission rates [23]. Each of the five geographic regions of Colombia is characterized by unique and seasonless weather patterns [24].

2. *Central port of entry.* The El Dorado International airport in Bogotá is by far the largest transportation hub for international travel, with nearly seven times the number of international travelers as the next largest airport in Colombia (with the majority of those travelers going to destinations in Latin America) [25]. This single, dominant point of entry for foreigners arriving from Europe and Asia means that the other points of entry are likely statistically insignificant as concerns the spread of SARS-CoV-2.

3. *Conditions favorable to rapid spread.* Colombian cities have high urban population densities (table 1) and public transportation is widely used by Colombians (roughly one fifth the number of registered cars per citizen versus the USA). For example, in Barranquilla, a coastal city in the Caribbean with hot temperatures, the average weekday commute time on public transportation is 77 minutes [26]. The heavy use of dense public transportation means that the measured lack of spread of the virus in this city is meaningful and not the result of some unique social distancing among the populace.

4. *Lack of air-conditioning.* Indoor air-conditioning is rare in Colombia [27]. The citizens live in the ambient conditions of temperature and humidity in his/her environment. This eliminates individual specific variation in temperature and humidity as a potential confounding factor.

5. *Swift and coordinated national response.* The first Covid-19 case was confirmed in Colombia on March 6, 2020 [28]. Nineteen days later, the government implemented a national quarantine, with tight cooperation at the local level and all testing orchestrated centrally through Bogotá, using uniform national guidelines [29]. This strong, centralized and swift action of the national government to the Covid-19 pandemic greatly simplifies the analysis because the data neatly separates in time into pre-quarantine and post-quarantine periods.

We call the rate at which SARS-CoV-2 was introduced into a city the *drip rate*. While the drip rate among the various regions of Colombia is unknown, the dominant port of entry (Bogotá) for international travel constrained the way the disease spread through the country. Furthermore, the heavy use of public transportation for inter- and intracity travel ensured that the disease spread quickly throughout the country, even to regions with low tourism.

Ostensibly, variations in the drip rate confound the analysis since cities with more tourism are likely to have received a higher influx of infected individuals. However, as we will show, the drip rate can be factored out of the analysis because it does not affect the rate at which the disease spreads. In contrast to the detection rate, the drip rate does not affect the exponent of disease growth (see methods and

supplementary information for more discussion on the drip rate).

Our data model considers both dynamic detection rates and variations in the drip rate between cities (see section 3.1). From this model, we derive a measure of disease transmission that is independent of both the drip rate and the overall detection rate (equation 5). By combining Colombian city-data with our drip model, we have largely mitigated the confounding factors (1-3) above and were able to identify a significant attenuation in transmission in hot cities with simultaneous moderate relative humidity.

2 The transmission of respiratory viruses

In this article, we do not consider the microscopic details of viral spread since there are too many variables to consider (e.g. turbulent airflow on buses). However, we briefly review some features and findings of recent models as they pertain to our assumptions [30] [31] [32] [33] [34] [35] [36].

First, we follow other researchers in using models of influenza to inform models of coronavirus, since seasonality is strongly correlated with infection rates in both diseases [37]. The most common environmental factors affecting airborne respiratory virus transmissions are (1) higher air transmission rates when the environment supports it (2) a strong spatial decline (i.e. Gaussian) in the transmission rate with the distance between the recipient and the diseased host (3) environmental factors such as air flow, temperature and humidity.

The strong dependence of the probability of transmission on host-recipient distance underscores the need to separate the data into pre-quarantine and post-quarantine segments since the degree of social distancing changed dramatically after quarantine was in place. Without this division, we would have to consider a time-dependent transmission rate, which unnecessarily complicates the analysis. Furthermore, different regions had different levels of compliance with the quarantine, and may have different economic factors (e.g. food factories) that lead to different transmission rates post-quarantine.

Following Herfts [38], we divide the transmission process into four basic steps: (1) a potential infectee interacts with the environment of an infectious host (2) the infectious host transmits an *intact* virus to the infectee (3) the virus infects the potential infectee (4) the virus replicates sufficiently for the infectee to become infectious.

In step (1), interaction, it is not necessary that the recipient and donor are in the "infective region" at the same time. With influenza-like diseases, virus-

droplets can remain suspended in the air for several hours in a suitable environment. An infectious host can also deposit the virus onto some surface that the potential infectee later touches.

In step (2), transmission, there is a timescale of virus viability that depends upon the environment. Influenza and SARS-CoV-2 are both enveloped by lipid-membranes derived from the budding host cell. The accumulation of damage to this membrane at higher temperatures may contribute to virus instability and decomposition.

The probability of infection, step (3), depends upon the number of intact viruses that deposit on the potential infectee and the susceptibility of the infectee. Susceptibility to infection depends on many factors, including age, medical history, obesity and even internal humidity, as a dry respiratory tract is more prone to infection [39].

In step (4), replication, both demographic and environmental factors play a role and temperature correlates with viral titer (hotter temperatures producing less titer) [33].

The rates, or probabilities, of these steps are not independent. Environmental factors influence the frequency and conditions under which people associate. Likewise, they regulate virus decomposition rates, modulate host susceptibility and the severity of infections within hosts. Finally, droplet settling times, droplet evaporation times, viral stability times, all depend on environmental factors such as humidity, temperature, wind etc.

To minimize the effects of these factors, it is essential to restrict the analysis to situations where the transmission occurs in environmental, social and economic steady-state conditions. The Colombian data meets these conditions because of (1) the lack of seasonality, resulting in nearly constant weather patterns in each region; (2) the widespread daily use of transportation in densely packed buses and subways; (3) the high population density in cities and (4) the suddenness and totality of the imposed quarantine.

Since cities differ in many ways, identifying the key variables (e.g. weather) responsible for variations in infection rates among cities is complicated. However, following research on influenza and coronavirus [37], we assume that averaging over populations sufficiently reduces the impact of all factors except population, public transportation usage, and weather. Apart from these, we will assume that the cities have roughly the same average demographic, economic and social conditions so that these variables do not confound our results. Consequently, we will assume that although transmission rates in different regions may be different, the overall transmission rate within each city is constant.

3 Methods

3.1 drip model

A significant fraction of infective hosts of SARS-CoV-2 are asymptomatic [8] [9] [10] [11] [12] [13] [14]. In addition, SARS-CoV-2 has a long incubation period of up to ~ 15 days [15]. During this time, the disease host is infectious but asymptomatic. In Colombia, international travel was banned three days after the imposition of national quarantine [28], thus we approximate that the rate at which infectious travelers arrived in each city was roughly constant over the pre-quarantine period.

We model the daily arrival of SARS-CoV-2 into each city as a Poisson process with mean I. That is, we assume that each day prior to the quarantine, $I[t]$ infected travelers arrive into a city where they begin infecting locals. We assume that on average, an infectious person infects r people each day, who in turn become infective (able to infect others) in one day. That is, on day t there are $I[t]$ new infectious arrivals, as well as the $N[t-1]$ total infectious people from the day before, and the $rN[t-1]$ people they infected (equation 1).

$$N[t] = N[t-1](1+r) + I[t] \tag{1}$$

This difference equation can easily be solved. We find that the expected number of infections on day t is:

$$\bar{N}[t] = I(1+1/r)(1+r)^t - I/r \tag{2}$$

Equation (1) gives the expected number of infections in a given city on day t. In our analysis, we allow both I, the drip rate, and r, the transmission rate, to vary by city.

While the disease is spreading, an infrastructure is being established to detect the disease which results in a dynamic disease detection rate. As a simple but useful case, consider a logistic increase in the detection rate. In supplementary information, we will consider more complicated models. We define the total probability of detecting an arbitrary infectious disease host on day t as:

$$p[t] = \frac{p_f}{1+e^{-k(t-h)}} \tag{3}$$

The detection rate increases from a small value ($p(0) = p_f/(1+e^{kh})$) at rate k, to a final detection capacity of p_f with half capacity reached on day h. The probability

of detecting c cases of SARS-CoV-2 on day t is distributed as a Binomial distribution $B(N[t], p(t), c(t))$. The average (expected) number of infections detected on day t is then:

$$\bar{c}[t] = N[t]p[t] \tag{4}$$

When r is small (which covers all cases of interest), the time-derivative of the log of the expected number of confirmed cases (the expected case log-velocity) is:

$$\boxed{\frac{d \log \bar{c}}{dt} \approx \frac{r}{1 - e^{-rt}} + \frac{k}{1 + e^{k(t-h)}}} \tag{5}$$

Note that the drip rate (I) and the overall detection rate (p_f) have fallen out. Equation (5) is the basic equation that we use to fit the data. However, we do not restrict our analysis to a logistic form for the increase in the detection rate (see supplementary materials).

3.2 data

We downloaded the case history for Colombia from the *Instituto Nacional de Salud* (`https://www.ins.gov.co/Noticias/Paginas/Coronavirus.aspx`). Next, we downloaded the weather for all of the cities in Colombia from World Weather Online (`https://www.worldweatheronline.com/`). Then we downloaded population data for Colombia from City Population dot de (`https://citypopulation.de/`).

3.3 data analysis

In order to apply equation 5 to the data, we first approximated the expected count number from the daily count number by computing a weighted average over neighboring days. That is, we smoothed the raw case number data for each city with a seven day triangle function. Next, we calculated the numerical derivative of $\log \bar{c}[t]$. Then we fit this log-velocity to the drip model by equation (5) as discussed in the supplementary information. This fit results in an error volume $e(r, k, h)$ that measures the error between the model under (r, k, h) and the transformed data. Since the computation of the log velocity is non-linear and our fit error function is non-linear, we cannot compute standard statistics on the quality of the fit. This is the price we pay for removing the drip rate and the overall detection rate from our model. Instead, we quantify the variation in the quality of the fits by the percent

increase from the global minimum. See figures 4 and 5 and the supplementary information for more details, including Python code to conduct the fits.

In order to divide the data into pre-quarantine and post-quarantine times, we analyzed the detection rate in Bogotá (see figure 2). By subtracting the infection log-velocity from the count log-velocity in equation (5) we obtained a free-form estimate of the detection rate in Bogotá. Since our model assumes a constant transmission rate, the decline in transmission of SARS-CoV-2 induced by the quarantine shows up as a decline in the detection rate, which we observe on April 3, 2020 (figure 2). From this date, we compute a threshold of April 7, 2020 for the remainder of cities throughout the country (Bogotá entered into quarantine 4 days prior[28]). Research estimates that Covid-19 can incubate for up to ~ 15 days, with a mean incubation period from $5-7$ days [15]. Additionally a three day delay between clinical presentation and diagnostic confirmation of Covid-19 was typical around this time.

4 Results and discussion

4.1 results

Inferring the rate of disease spread from daily case numbers can be deceptive, since variations in the disease detection rate and the drip rate result in detection of significantly larger or smaller fractions of the disease population. To account for this and other factors, we developed the drip model which removes the overall detection rate. Since the data span about 30 days, exponential growth will only be manifest for cities with transmission rates significantly greater than $1/30 \sim 0.033$. We consider 0.05 to be the minimum threshold on the transmission rate for observing exponential growth in a city. We associate transmission rates above this threshold with airborne transmission and transmission rates below this threshold with tourism and direct transmission [40].

The data only show clear exponential growth in large cities with humidity over 80% and mean maximum daily temperatures below 30 degrees Celsius (Bogotá, Cali, and Medellín). The humidity in these cities is roughly the same (82 %), and they have similar total populations and urban population densities (table 1). The transmission rate declines among these cities with increasing temperature. Since these cities had the largest number of confirmed cases of Covid-19, these fits have the highest confidence.

We note that none of the smaller cities at any temperature and humidity regis-

tered significant transmission rates in the pre-quarantine data. For example, Soacha and Bucaramanga compare to Bogotá and Medellín respectively. Soacha shares climate with Bogotá but has one tenth the total population (Soacha and Bogotá are neighboring cities and are connected by urban rail). Soacha has a higher urban population density than Bogotá. Bucaramanga has nearly one-fifth the population of Medellín (at similar temperature and humidity) and half the population density. Bogotá is more than 10 times larger than Soacha and Medellín more than twice as large as Bucaramanga. Moreover, Bogotá and Medellín are regional transportation hubs. Thus we conclude that the lack of transmission in Soacha and Bucaramanga is attributable to transportation factors as governed by total population and regional importance.

As we were preparing this manuscript, we observed an outbreak in Cartagena de Indias, a hot city in the Caribbean coast that had exhibited low case numbers for over two months. This outbreak began about 50 days into the quarantine and showed a higher transmission rate than at any previous time in Cartagena and thus suggests that the outbreak could not be solely attributable to quarantine violations. Since international travel had been banned and intercity travel highly restricted for nearly 50 days prior to the outbreak, we conclude that the outbreak must reflect a change in environment.

While the weather in Colombia is nearly constant, there are small temperature and humidity shifts associated with rainy and dry seasons. This outbreak, and several other smaller outbreaks, exhibits a remarkable correlation with sustained humidity above about 78%. Based upon the fact that (1) this outbreak occurred during quarantine and (2) international travel was banned and local travel highly restricted for 50 days prior to the outbreak and (3) temperature was nearly constant prior to the outbreak and (4) there was no observable spike in testing around the outbreak, we conclude that this outbreak was driven by relative humidity (see figure 6).

Finally, we note that lack of rainfall appears to offer additional protection from Covid-19 outbreaks. Rainfall has been identified as a correlate of influenza outbreaks in the tropics [41] [42], likely due to increased crowding from sudden tropical storms [42]. Additional weather variables such as hours per day of sunlight, UV, etc., also show some correlation with our data. A post-quarantine analysis, and likely an analysis with international data, will be needed to establish all of the weather factors on Covid-19 outbreaks.

4.2 mechanism considerations

Our analysis focuses upon the pre-quarantine dynamics of Covid-19 in Colombia. During this time, the humidity and temperature was nearly constant by region and we assume social and economic steady state conditions. We observed a clear separation of the data according to three variables: total population, temperature, and relative humidity. Cities with populations significantly under 1 million did not exhibit any significant outbreak of Covid-19. Large cities with warm weather (maximum daily temperature above 30 degrees Celsius) and simultaneous moderate humidity (below 78%) did not experience outbreaks and showed transmission rates consistent with tourism and direct contact. Large cities with high humidity (above 80%) experienced significant outbreaks, with transmission rates that declined with increasing temperature.

Cartagena de Indias, a hot Caribbean city that showed very low transmission rates for March and April, experienced an outbreak in early May consistent with high transmission rates. This outbreak followed a sustained rise in daily mean humidity above 80%, a threshold that has been previously identified as favorable to enveloped viruses.

Comodulation of viral infectivity by temperature and by humidity has been experimentally demonstrated in a variety of enveloped viruses [43] such as SARS-CoV [44], influenza [45] [46] [34] [47] [48] and SARS-CoV-2 [49] (for temperature only) and other enveloped viruses [50]. Three chief mechanisms have been proposed to explain the role of temperature and humidity upon enveloped viruses: (1) destabilization of the virus within the droplet-matrix [45] [51] (2) evaporation and settling of virus droplets [36] [51] and (3) reduced viral titer produced by the host at higher temperatures [33].

Reduced viral titer could account for some of the reduced transmission observed at higher temperatures. Halloran et al show a reduction in peak nasal titer for influenza of an order of magnitude between 5 and 30 degrees Celsius in guinea pigs [33]. However, viral titer cannot explain the outbreak in Cartagena which appears to be driven entirely by relative humidity; it is improbable that small variations in ambient humidity could affect viral titer given that the air within the human respiratory system is saturated and unlikely to vary with small changes in ambient RH [52].

The timescale of temperature-only destabilization in solution appears to be on the order of minutes [45] [50] [49], although direct measurements at shorter timescales in conditions that mimic respiratory droplets are lacking [51]. Droplet

settling timescales vary between minutes and hours depending upon droplet size [51]. Given the dense packing on public transportation of cities with attenuated transmission, we reason that the mechanism behind this attenuation must act on the timescale of seconds [53] [33] and thus rule out droplet settling and temperature-only viral destabilization.

Airborne respiratory droplets evaporate down to half size in about one second [51] [46]. This evaporation is thought to influence viral stability through salt and protein concentrations, pH gradients, and surface sheering [46]. Humidity and temperature both influence droplet evaporation, with temperature influencing the rate and relative humidity determining the final droplet size [33]. While the timescale of droplet shrinkage has been studied, the timescale of viral inactivation within the shrunken and toxic respiratory droplets is, to our knowledge, unknown [51]. Determining this timescale could have important implications for policy surrounding the Covid-19 pandemic, since fast destabilization at specific temperature and humidity intervals would have both prevention and therapeutic implications. Thus experiments are needed to resolve the impact of temperature and humidity upon the infectivity of SARS-CoV-2 within respiratory droplets.

5 Conclusion

We observed attenuated transmission of SARS-CoV-2 at high temperatures and simultaneous moderate humidity. High humidity permits transmission even where the temperatures are high, consistent with models of viral destabilization by droplet evaporation. Our observations forecast a decline in the spread of SARS-CoV-2 with temperature for regions with moderate humidity. As in the case of Cartagena, outbreaks are possible in hot regions if the humidity climbs above 78%. If laboratory experiments confirm our hypothesis that viral infectivity is comodulated by temperature and by humidity, then there are several implications surrounding the Covid-19 pandemic. First, indoor climate control (or lack thereof) might be considered as a means of mitigating the spread of SARS-CoV-2. Secondly, the same mechanisms of viral destabilization within evaporated respiratory droplets could be considered as means of directly combating the virus [54] [55] [56]. Of particular importance is establishing the timescale of viral destabilization within respiratory droplets as a function of temperature and humidity, resolved on the shortest timescale possible.

In conclusion, we analyzed the pre-quarantine dynamics of the spread of SARS-CoV-2 in Colombia and found an attenuation in transmission for temperatures above 30 degrees Celsius when the mean humidity was simultaneously below 75%. We ob-

served an outbreak in Cartagena that closely followed sustained humidity above 78%. Given the over-crowded public transportation systems and high urban population densities of cities with highly attenuated transmission, we hypothesize that the attenuation is caused by rapid viral inactivation within the droplet matrix as mediated by evaporation through temperature and relative humidity, with direct temperature effects upon the virus contributing. Laboratory experiments to establish the variation in infectivity of SARS-CoV-2 within respiratory droplets as a function of temperature and humidity, and the timescale of the inactivation, could have significant implications for policy surrounding the COVID-19 pandemic.

6 Figures

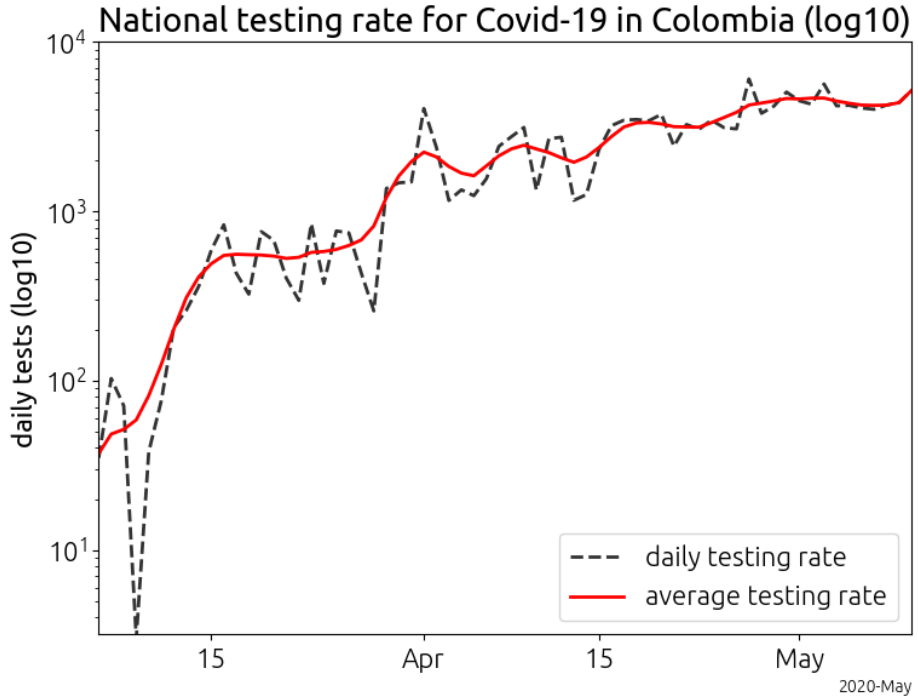

Figure 1: Testing rates with time in Colombia, March through early May. The daily number of tests conducted for SARS-CoV-2 increased by two orders of magnitude from March through May 2020. We have identified dynamic testing rates as a key confounding factor in the analysis of Covid-19 case data.

	population	pop. density	max. daily temp	daily humidity
Bogotá	7,387,400	19,475	20.7	82
Medellín	2,382,399	20,681	26.0	83
Cali	2,172,527	16,247	27.0	81
Barranquilla	1,205,284	14,455	32.3	68
Cartagena	876,885	17,053	30.1	74

Table 1: Geographic and population data for the five largest cities in Colombia. The temperature and humidity are averages taken over the month of March, 2020. The population density is the urban population density.

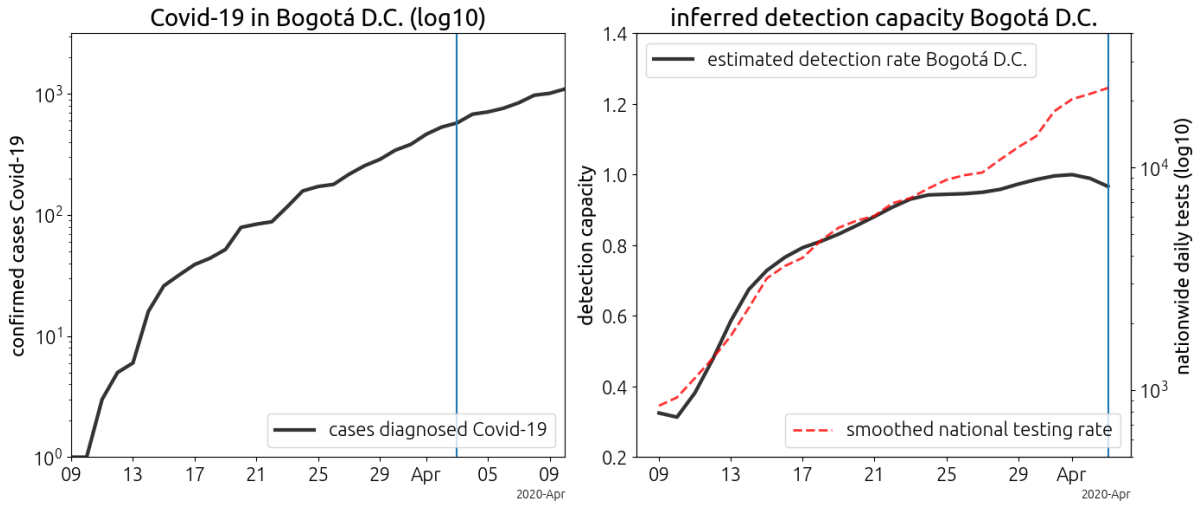

Figure 2: (Left panel) The number of confirmed cases of Covid-19 in Bogotá, Colombia from March 9 to April 10 2020 (log base 10). (Right panel) The detection rate in Bogotá deduced by our algorithm. Since the transmission rate is constrained to a constant, the reduction in the transmission rate induced by the quarantine shows up in our model as a decrease in the detection rate (red vertical line). The vertical bar on April 3, 2020 denotes a combination of the impact of the quarantine on the spread of SARS-CoV-2 in Bogotá and a brief decline in the testing rate. Since Bogotá went into quarantine 4 days before the rest of the country, the pre-quarantine data ends April 7, 2020. Note we have plotted the smoothed national testing rate in dashed red; this plot is on a log10 scale and only serves to show qualitative agreement between the inferred detection rate and the daily testing rate. The national testing rate includes testing for all cities in Colombia.

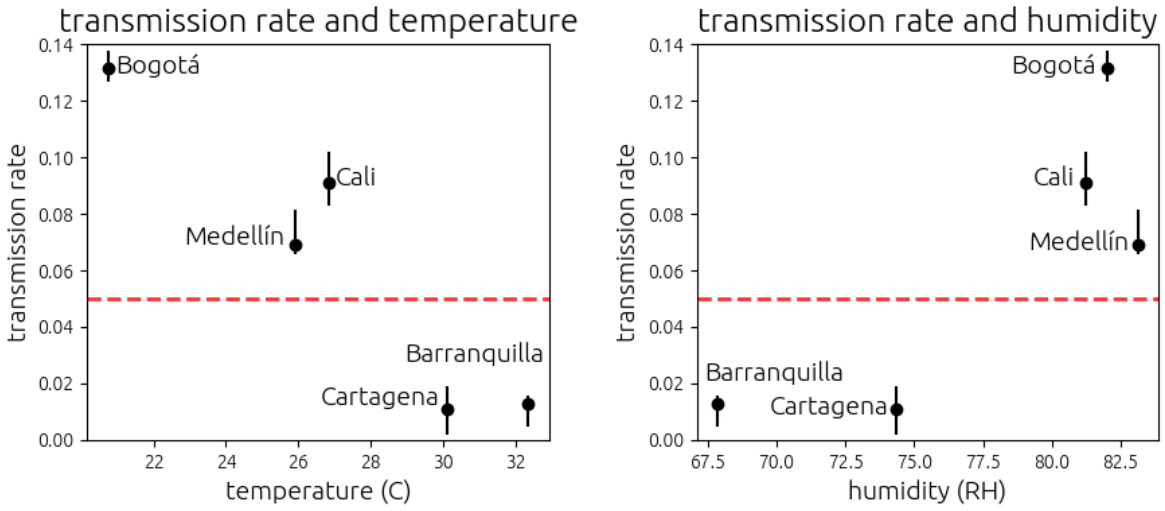

Figure 3: Transmission rate with temperature and humidity for the five largest cities in Colombia. (left) The transmission rate of a city is plotted against the mean maximum daily temperature of the city during the pre-quarantine period. The dashed red line denotes the transmission threshold of 0.05. We associate transmission rates above this threshold with airborne transmission and transmission rates below this threshold with tourism and direct transmission. The error bar on each city denotes values of the transmission rate that correspond to less than a 10% rise in the fit error function. (right) Same as (left) but for relative humidity.

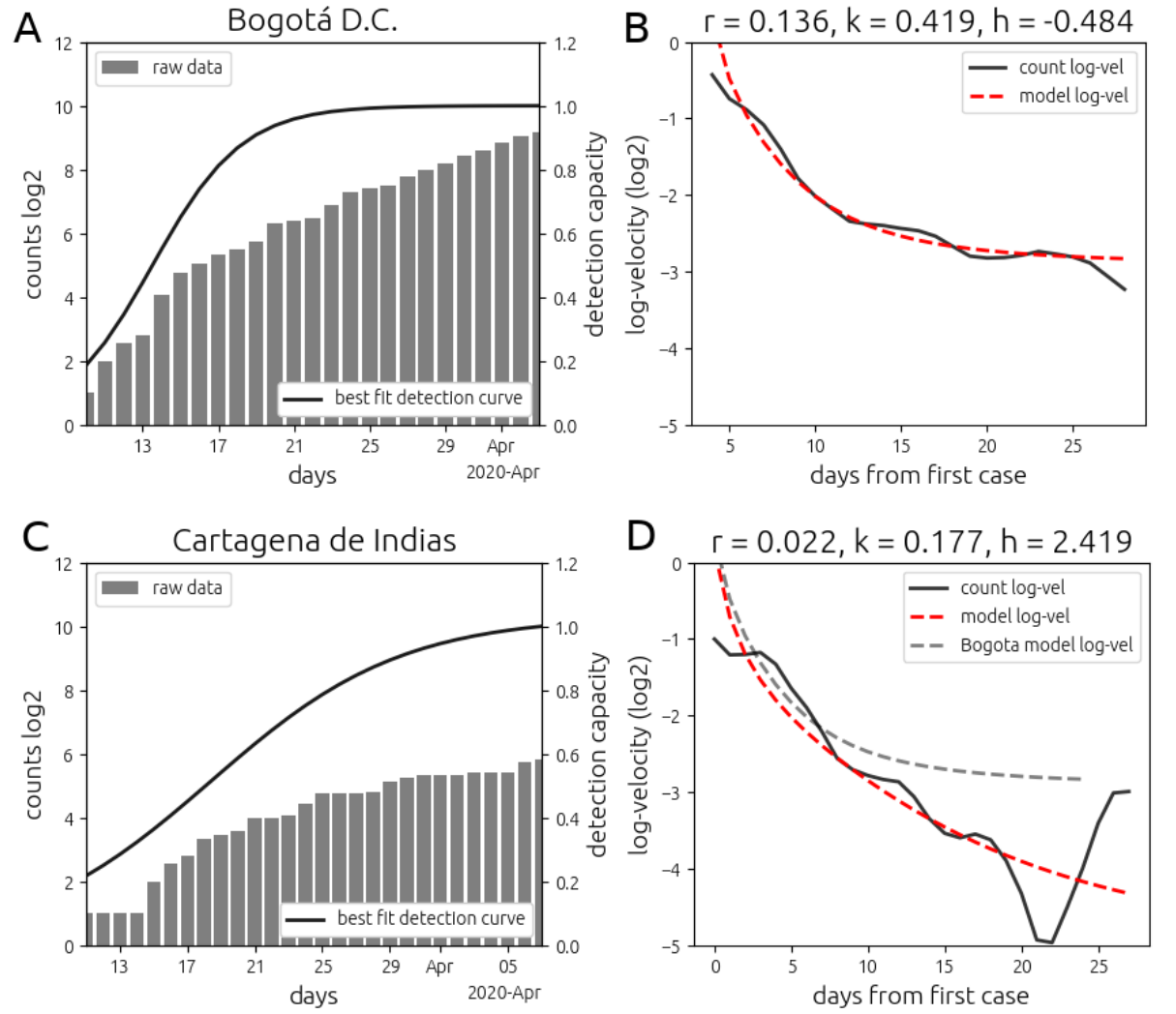

Figure 4: Best fits, Bogotá D.C. and Cartagena de Indias pre-quarantine. **A**. We plot the case numbers in Bogotá (gray bars) along with their adjusted values after accounting for detection (dashed red). In black, we plot the best-fit detection curve obtained. **B**. We plot the numerical (black) log-velocity for the Bogotá data as well as the best-fit model (dashed red). **C**. Same as **A** but for Cartagena, where the average maximum daily temperature is 30 degrees Celsius. **D**. Same as **B** but for Cartagena. Note the rapid increase in cases registered in Cartagena at the end of March show up in our model as in increase in detection. Indeed, the Colombian testing rate data shows nearly a doubling in the test rate between March 27 and March 30. We have included the best fit for Bogotá as a comparison (dashed gray). This fit is rendered even more implausible by detection considerations.

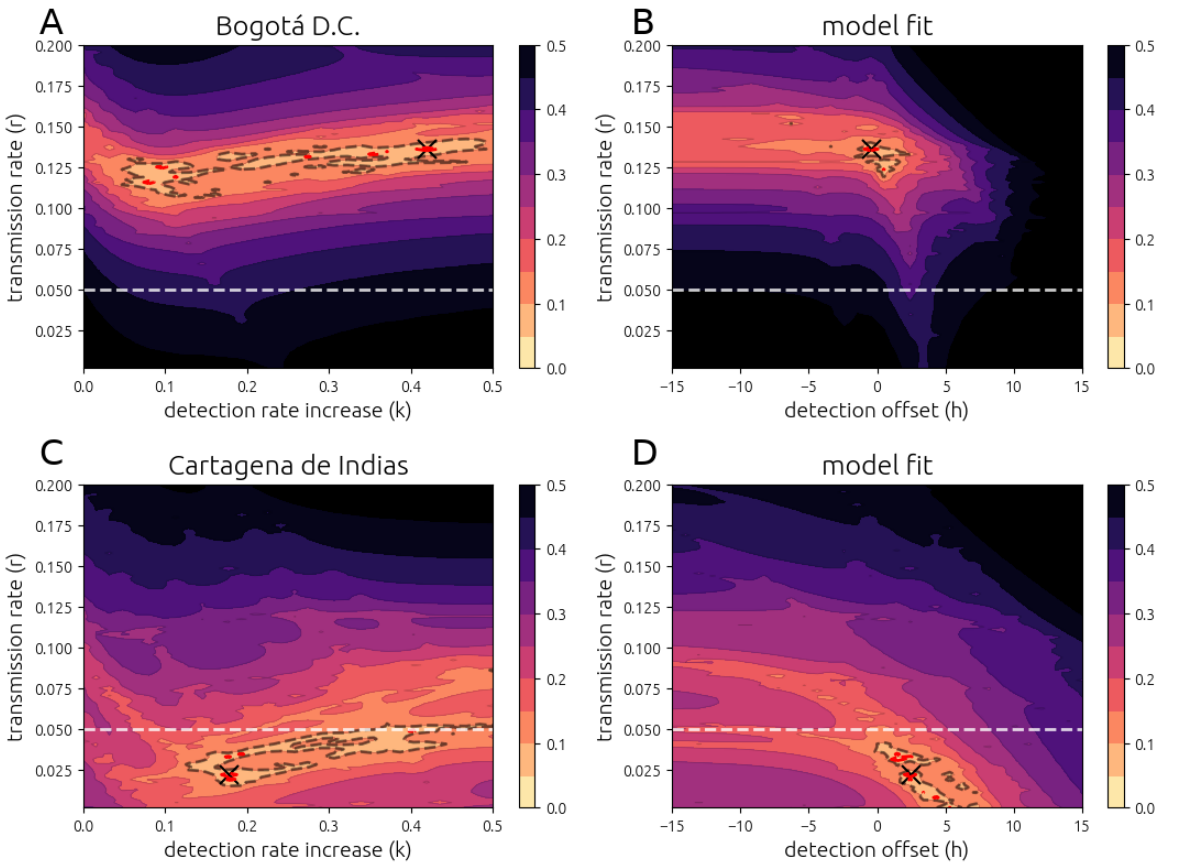

Figure 5: Fit variation, Bogotá D.C. and Cartagena de Indias, pre-quarantine. All surfaces show cross-sections of the error function $e(r, k, h)$ between the model under parameters (r, k, h) and the transformed data. The error bars are given in terms of percent increase from the global minimum. Global minima are denoted by a black cross. The dashed white line indicates the threshold $r = 0.05$ for observing clear exponential growth in our model. The red contours denote an increase from the global minimum of 5% and the gray contours denote an increase from the global minimum by 10% **A** Bogotá D.C. The surfaces shows the error function with h fixed at the global minimum. **B** Bogotá D.C. The surfaces shows the error function with k fixed at the global minimum **C** Cartagena de Indias. The surfaces shows the error function with h fixed at the global minimum. **D** Cartagena de Indias. The surfaces shows the error function with k fixed at the global minimum.

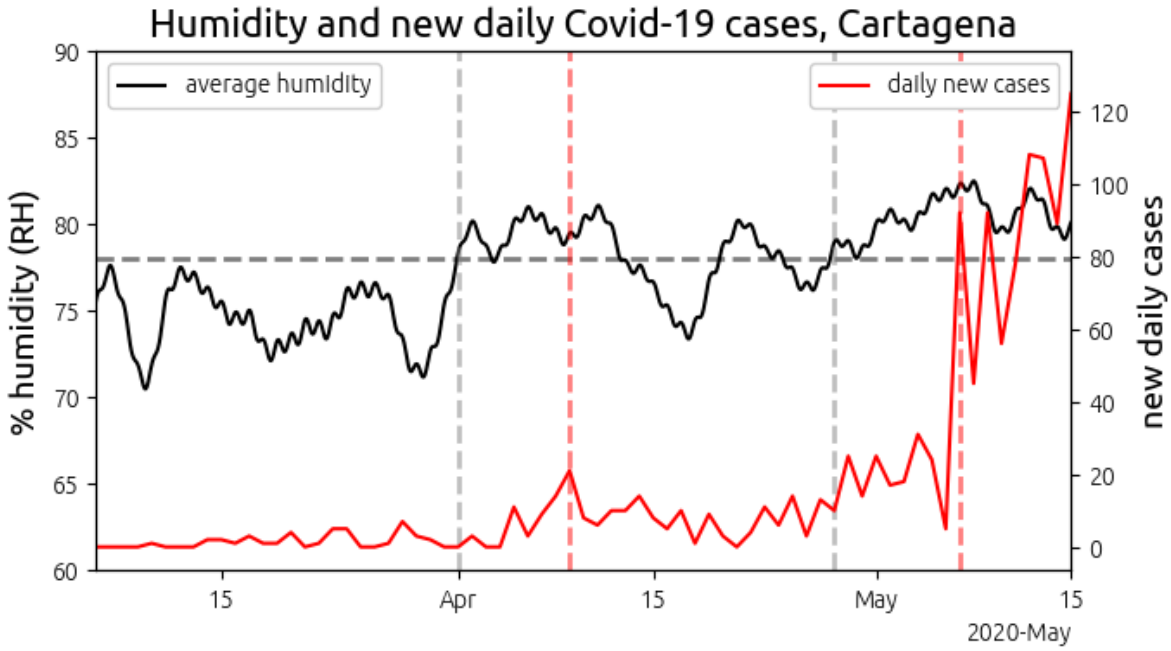

Figure 6: Outbreak in Cartagena de Indias. After two months of a daily case count of around 10, the case count in Cartagena spiked by nearly an order of magnitude in the beginning of May. The solid black line plots the average daily humidity in Cartagena (left axis). The solid red line plots the number of new cases of Covid-19 diagnosed in Cartagena as a function of time (right axis). The horizontal dashed gray line plots a mean humidity level of 78%. The vertical dashed gray bar on the left denotes April 1, 2020, the first day that Cartagena experienced mean humidity of 78% since the first recorded case of Covid-19 in Colombia. On April 9, 2020, denoted by the first vertical dashed red line from the left, 8 days after the humidity increase, a spike in Covid-19 cases was registered. The second vertical dashed gray bar denotes April 28, the beginning of the second sustained period of humidity above 78% in Cartagena. A major outbreak was soon observed beginning roughly May 7, 2020, second vertical dashed red bar from the left, 9 days after the humidity rise.

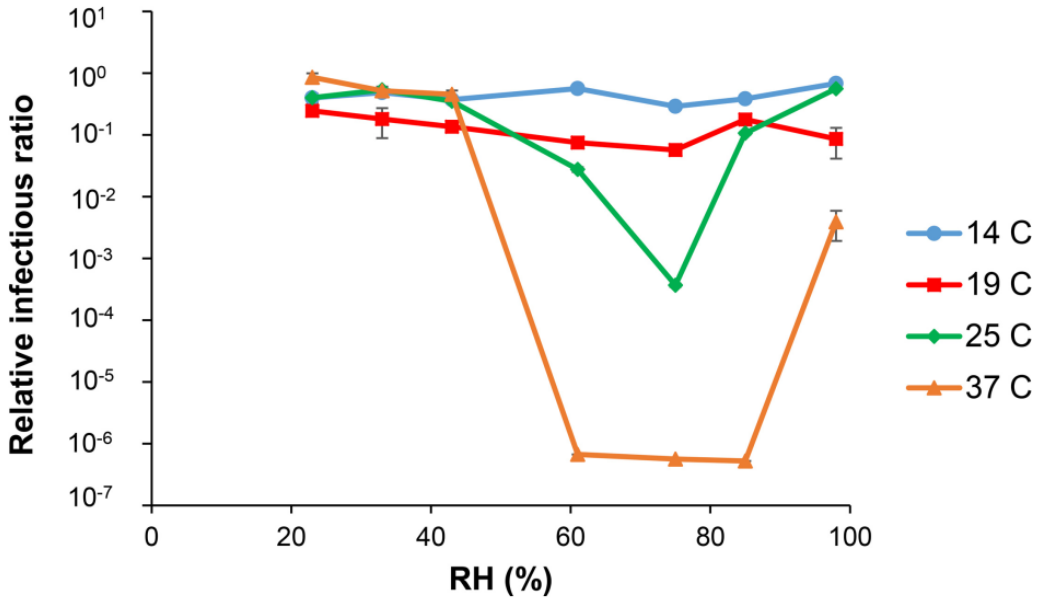

Figure 7: Original data from Prussin et al [50] on the relationship between temperature, RH and Phi6 infectivity. Phi6 is an enveloped virus used a model for influenza, coronavirus and other respiratory viruses. The error bars are shown but too small to be visible in the figure.

References

[1] S. Su, G. Wong, W. Shi, J. Liu, A. C. Lai, J. Zhou, W. Liu, Y. Bi, and G. F. Gao, "Epidemiology, genetic recombination, and pathogenesis of coronaviruses," *Trends in microbiology*, vol. 24, no. 6, pp. 490–502, 2016.

[2] M. M. Lai and D. Cavanagh, "The molecular biology of coronaviruses," in *Advances in virus research*, vol. 48, pp. 1–100, Elsevier, 1997.

[3] J. A. Al-Tawfiq, "Asymptomatic coronavirus infection: Mers-cov and sars-cov-2 (covid-19)," *Travel Med Infect Dis*, vol. 101608, 2020.

[4] J. Helms, S. Kremer, H. Merdji, R. Clere-Jehl, M. Schenck, C. Kummerlen, O. Collange, C. Boulay, S. Fafi-Kremer, M. Ohana, *et al.*, "Neurologic features in severe sars-cov-2 infection," *New England Journal of Medicine*, 2020.

[5] P. Sun, S. Qie, Z. Liu, J. Ren, and J. J. Xi, "Clinical characteristics of 50466 patients with 2019-ncov infection," *medRxiv*, 2020.

[6] Z. Xu, L. Shi, Y. Wang, J. Zhang, L. Huang, C. Zhang, S. Liu, P. Zhao, H. Liu, L. Zhu, *et al.*, "Pathological findings of covid-19 associated with acute respiratory distress syndrome," *The Lancet respiratory medicine*, vol. 8, no. 4, pp. 420–422, 2020.

[7] W.-j. Guan, Z.-y. Ni, Y. Hu, W.-h. Liang, C.-q. Ou, J.-x. He, L. Liu, H. Shan, C.-l. Lei, D. S. Hui, *et al.*, "Clinical characteristics of coronavirus disease 2019 in china," *New England journal of medicine*, vol. 382, no. 18, pp. 1708–1720, 2020.

[8] Y. Liu, A. A. Gayle, A. Wilder-Smith, and J. Rocklöv, "The reproductive number of covid-19 is higher compared to sars coronavirus," *Journal of travel medicine*, 2020.

[9] X. Pan, D. Chen, Y. Xia, X. Wu, T. Li, X. Ou, L. Zhou, and J. Liu, "Asymptomatic cases in a family cluster with sars-cov-2 infection," *The Lancet Infectious Diseases*, vol. 20, no. 4, pp. 410–411, 2020.

[10] C. Rothe, M. Schunk, P. Sothmann, G. Bretzel, G. Froeschl, C. Wallrauch, T. Zimmer, V. Thiel, C. Janke, W. Guggemos, *et al.*, "Transmission of 2019-ncov infection from an asymptomatic contact in germany," *New England Journal of Medicine*, vol. 382, no. 10, pp. 970–971, 2020.

[11] A. Kimball, "Asymptomatic and presymptomatic sars-cov-2 infections in residents of a long-term care skilled nursing facility—king county, washington, march 2020," *MMWR. Morbidity and mortality weekly report*, vol. 69, 2020.

[12] X. Jiang, S. Rayner, and M.-H. Luo, "Does sars-cov-2 has a longer incubation period than sars and mers?," *Journal of medical virology*, 2020.

[13] W. E. Wei, Z. Li, C. J. Chiew, S. E. Yong, M. P. Toh, and V. J. Lee, "Presymptomatic transmission of sars-cov-2—singapore, january 23–march 16, 2020," *Morbidity and Mortality Weekly Report*, vol. 69, no. 14, p. 411, 2020.

[14] R. Li, S. Pei, B. Chen, Y. Song, T. Zhang, W. Yang, and J. Shaman, "Substantial undocumented infection facilitates the rapid dissemination of novel coronavirus (sars-cov-2)," *Science*, vol. 368, no. 6490, pp. 489–493, 2020.

[15] C. Leung, "The difference in the incubation period of 2019 novel coronavirus (sars-cov-2) infection between travelers to hubei and nontravelers: the need for a longer quarantine period," *Infection Control & Hospital Epidemiology*, pp. 1–3, 2020.

[16] D. Wu, T. Wu, Q. Liu, and Z. Yang, "The sars-cov-2 outbreak: what we know," *International Journal of Infectious Diseases*, 2020.

[17] W. H. Organization *et al.*, "Coronavirus disease 2019 (covid-19): situation report, 72," 2020.

[18] J. H. Tanne, E. Hayasaki, M. Zastrow, P. Pulla, P. Smith, and A. G. Rada, "Covid-19: how doctors and healthcare systems are tackling coronavirus worldwide," *Bmj*, vol. 368, 2020.

[19] D. Fisher and A. Wilder-Smith, "The global community needs to swiftly ramp up the response to contain covid-19," *The Lancet*, vol. 395, no. 10230, pp. 1109–1110, 2020.

[20] R. Lassaunière, A. Frische, Z. B. Harboe, A. C. Nielsen, A. Fomsgaard, K. A. Krogfelt, and C. S. Jørgensen, "Evaluation of nine commercial sars-cov-2 immunoassays," *Medrxiv*, 2020.

[21] W. H. Organization *et al.*, "Management of ill travellers at points of entry–international airports, seaports and ground crossings–in the context of covid-19 outbreak: interim guidance, 16 february 2020," tech. rep., World Health Organization, 2020.

[22] F. Sánchez and J. N. Méndez, *Geography and economic development: A municipal approach for Colombia.* Centro de Estudios Sobre Desarrollo Economico, Universidade de los Andes, 2000.

[23] J. Tan, L. Mu, J. Huang, S. Yu, B. Chen, and J. Yin, "An initial investigation of the association between the sars outbreak and weather: with the view of the environmental temperature and its variation," *Journal of Epidemiology & Community Health*, vol. 59, no. 3, pp. 186–192, 2005.

[24] J. A. Fernández-Niño, V. A. Flórez-García, C. I. Astudillo-García, and L. A. Rodríguez-Villamizar, "Weather and suicide: A decade analysis in the five largest capital cities of colombia," *International journal of environmental research and public health*, vol. 15, no. 7, p. 1313, 2018.

[25] A. C. D. COLOMBIA, "Estadisticas trafico de aeropuertos enero 2019." `http://www.aerocivil.gov.co/atencion/estadisticas-de-las-actividades-aeronauticas/_layouts/15/WopiFrame.aspx?sourcedoc=/atencion/estadisticas-de-las-actividades-aeronauticas/Estadsticas%20operacionales/Estadisticas%20Trafico%20de%20Aeropuertos%20Enero%202019.xls&action=default`. Accessed: 2020-05-12.

[26] moovit app, "Statistics on public transportation usage in barranquilla." `https://moovitapp.com/insights/en/Moovit_Insights_Public_Transit_Index_Colombia_Barranquilla-2883`. Accessed: 2020-05-01.

[27] O. Ortiz, F. Castells, and G. Sonnemann, "Operational energy in the life cycle of residential dwellings: The experience of spain and colombia," *Applied Energy*, vol. 87, no. 2, pp. 673–680, 2010.

[28] A. M. O. Tono, M. García, C. J. Moncayo, C. Wills, and Á. M. C. Mahecha, "Covid-19: generalidades, comportamiento epidemiológico y medidas adoptadas en medio de la pandemia en colombia," *ACTA DE OTORRINOLARINGOLOGÍA & CIRUGÍA DE CABEZA Y CUELLO*, pp. 4–13, 2020.

[29] C. Ministerio de Salud, "Lineamientos para el uso de pruebas diagnÓsticas de laboratorio durante la pandemia del sars-cov-2 (covid-19) en colombia." `https://www.minsalud.gov.co/Ministerio/Institucional/Procesos%20y%20procedimientos/GIPS21.pdf`. Accessed: 2020-05-12.

[30] S. Chen, C. Chio, L. Jou, C. Liao, *et al.*, "Viral kinetics and exhaled droplet size affect indoor transmission dynamics of influenza infection," *Indoor Air*, vol. 19, no. 5, p. 401, 2009.

[31] R. Tellier, "Review of aerosol transmission of influenza a virus," *Emerging infectious diseases*, vol. 12, no. 11, p. 1657, 2006.

[32] C.-M. Liao, C.-F. Chang, and H.-M. Liang, "A probabilistic transmission dynamic model to assess indoor airborne infection risks," *Risk Analysis: An International Journal*, vol. 25, no. 5, pp. 1097–1107, 2005.

[33] S. K. Halloran, A. S. Wexler, and W. D. Ristenpart, "A comprehensive breath plume model for disease transmission via expiratory aerosols," *PloS one*, vol. 7, no. 5, 2012.

[34] K. Lin and L. C. Marr, "Humidity-dependent decay of viruses, but not bacteria, in aerosols and droplets follows disinfection kinetics," *Environmental Science & Technology*, vol. 54, no. 2, pp. 1024–1032, 2019.

[35] J. S. Kutter, M. I. Spronken, P. L. Fraaij, R. A. Fouchier, and S. Herfst, "Transmission routes of respiratory viruses among humans," *Current opinion in virology*, vol. 28, pp. 142–151, 2018.

[36] W. Yang and L. C. Marr, "Mechanisms by which ambient humidity may affect viruses in aerosols," *Appl. Environ. Microbiol.*, vol. 78, no. 19, pp. 6781–6788, 2012.

[37] M. Moriyama, W. J. Hugentobler, and A. Iwasaki, "Seasonality of respiratory viral infections," *Annual Review of Virology*, vol. 7, 2020.

[38] S. Herfst, M. Böhringer, B. Karo, P. Lawrence, N. S. Lewis, M. J. Mina, C. J. Russell, J. Steel, R. L. de Swart, and C. Menge, "Drivers of airborne human-to-human pathogen transmission," *Current opinion in virology*, vol. 22, pp. 22–29, 2017.

[39] A. Iwasaki, E. F. Foxman, and R. D. Molony, "Early local immune defences in the respiratory tract," *Nature Reviews Immunology*, vol. 17, no. 1, p. 7, 2017.

[40] A. Lowen and P. Palese, "Transmission of influenza virus in temperate zones is predominantly by aerosol, in the tropics by contact: a hypothesis," *PLoS currents*, vol. 1, 2009.

[41] R. P. Soebiyanto, F. Adimi, and R. K. Kiang, "Modeling and predicting seasonal influenza transmission in warm regions using climatological parameters," *PloS one*, vol. 5, no. 3, 2010.

[42] R. P. Soebiyanto, W. Clara, J. Jara, L. Castillo, O. R. Sorto, S. Marinero, M. E. B. de Antinori, J. P. McCracken, M.-A. Widdowson, E. Azziz-Baumgartner, *et al.*, "The role of temperature and humidity on seasonal influenza in tropical areas: Guatemala, el salvador and panama, 2008–2013," *PloS one*, vol. 9, no. 6, 2014.

[43] J. W. Tang, "The effect of environmental parameters on the survival of airborne infectious agents," *Journal of the Royal Society Interface*, vol. 6, no. suppl_6, pp. S737–S746, 2009.

[44] K. Chan, J. Peiris, S. Lam, L. Poon, K. Yuen, and W. Seto, "The effects of temperature and relative humidity on the viability of the sars coronavirus," *Advances in virology*, vol. 2011, 2011.

[45] J. Hemmes, K. Winkler, and S. Kool, "Virus survival as a seasonal factor in influenza and poliomyelitis," *Nature*, vol. 188, no. 4748, pp. 430–431, 1960.

[46] W. Yang, S. Elankumaran, and L. C. Marr, "Relationship between humidity and influenza a viability in droplets and implications for influenza's seasonality," *PloS one*, vol. 7, no. 10, 2012.

[47] I. V. Polozov, L. Bezrukov, K. Gawrisch, and J. Zimmerberg, "Progressive ordering with decreasing temperature of the phospholipids of influenza virus," *Nature chemical biology*, vol. 4, p. 248, 2008.

[48] J. D. Brown, G. Goekjian, R. Poulson, S. Valeika, and D. E. Stallknecht, "Avian influenza virus in water: infectivity is dependent on ph, salinity and temperature," *Veterinary microbiology*, vol. 136, no. 1-2, pp. 20–26, 2009.

[49] A. W. Chin, J. T. Chu, M. R. Perera, K. P. Hui, H.-L. Yen, M. C. Chan, M. Peiris, and L. L. Poon, "Stability of sars-cov-2 in different environmental conditions," *The Lancet Microbe*, vol. 1, no. 1, p. e10, 2020.

[50] A. J. Prussin, D. O. Schwake, K. Lin, D. L. Gallagher, L. Buttling, and L. C. Marr, "Survival of the enveloped virus phi6 in droplets as a function of relative humidity, absolute humidity, and temperature," *Appl. Environ. Microbiol.*, vol. 84, no. 12, pp. e00551–18, 2018.

[51] L. C. Marr, J. W. Tang, J. Van Mullekom, and S. S. Lakdawala, "Mechanistic insights into the effect of humidity on airborne influenza virus survival, transmission and incidence," *Journal of the Royal Society Interface*, vol. 16, no. 150, p. 20180298, 2019.

[52] J. E. Walker and R. E. Wells, "Heat and water exchange in the respiratory tract," *The American journal of medicine*, vol. 30, no. 2, pp. 259–267, 1961.

[53] L. Zhang and Y. Li, "Dispersion of coughed droplets in a fully-occupied high-speed rail cabin," *Building and Environment*, vol. 47, pp. 58–66, 2012.

[54] S. Bibby, S. Reddy, T. Cripps, S. McKinstry, M. Weatherall, R. Beasley, and J. Pilcher, "Tolerability of nasal delivery of humidified and warmed air at different temperatures: a randomised double-blind pilot study," *Pulmonary medicine*, vol. 2016, 2016.

[55] M. S. Nanda, "Efficacy of steam inhalation with inhalant capsules in patients with common cold in a rural set up," *IOSR Journal of Dental and Medical Sciences (IOSR-JDMS)*, 2015.

[56] C. Conti, A. De Marco, P. Mastromarino, P. Tomao, and M. Santoro, "Antiviral effect of hyperthermic treatment in rhinovirus infection," *Antimicrobial agents and chemotherapy*, vol. 43, no. 4, pp. 822–829, 1999.